J|A|C|S
ARTICLES
Published on Web 04/15/2006

Mechanism-Based Cofactor Derivatization of a Copper Amine Oxidase by a Branched Primary Amine Recruits the Oxidase Activity of the Enzyme to Turn Inactivator into Substrate

Chunhua Qiao,[†] Ke-Qing Ling,[†] Eric M. Shepard,[‡] David M. Dooley,[‡] and Lawrence M. Sayre*,[†]

Contribution from the Department of Chemistry, Case Western Reserve University, Cleveland, Ohio 44106, and Department of Chemistry and Biochemistry, Montana State University, Bozeman, Montana

Received January 10, 2006; E-mail: LMS3@case.edu

Abstract: The copper amine oxidases (CAOs) have evolved to catalyze oxidative deamination of *unbranched* primary amines to aldehydes. We report that a *branched* primary amine bearing an aromatization-prone moiety, ethyl 4-amino-4,5-dihydrothiophene-2-carboxylate (**1**), is recognized enantioselectively ($S \gg R$) by bovine plasma amine oxidase (BPAO) both as a temporary inactivator and as a substrate. Substrate activity results from an O_2-dependent turnover of the covalently modified enzyme, with release of 4-aminothiophene-2-carboxylate (**2**) as ultimate product. Interaction of (*S*)-**1** with BPAO occurs within the enzyme active site with a dissociation constant of 0.76 μM. Evidence from kinetic and spectroscopic studies, and HPLC analysis of stoichiometric reactions of BPAO with (*S*)-**1**, combined with a model study using a quinone cofactor mimic, establishes that the enzyme metabolizes **1** according to a transamination mechanism. Following the initial isomerization of substrate Schiff base to product Schiff base, a facile aromatization of the latter results in a metastable N-aryl derivative of the reduced cofactor aminoresorcinol, which is catalytically inactive. The latter derivative is then slowly oxidized by O_2, apparently facilitated partially by the active-site Cu(II), to form a quinonimine of the native cofactor that releases **2** upon hydrolysis or transimination with substrate amine. Preferential metabolism of (*S*)-**1** is consistent with the preferential removal of the *pro-S* α-proton in metabolism of benzylamine by BPAO. This study represents the first report of product identification in metabolism of a branched primary amine by a copper amine oxidase and suggests a novel type of reversible mechanism-based (covalent) inhibition where inhibition *lifetime* can be fine-tuned independently of inhibition *potency*.

Introduction

The copper amine oxidases (CAOs) catalyze the oxidative deamination of primary amines to aldehydes at the expense of reduction of O_2 to H_2O_2, through an active-site trihydroxyphenylalanine quinone (TPQ) cofactor-mediated pyridoxal-like transamination process.[1,2] The key step (Scheme 1, path A) involves an active-site base-mediated C_α deprotonation, accomplishing tautomerization of substrate Schiff base (SSB) to product Schiff base (PSB), which hydrolyzes to release aldehyde and generate the reduced aminoresorcinol form of the cofactor (TPQ_{amr}). The latter is subsequently reoxidized to the starting quinone with release of NH_3. The transamination chemistry has been recapitulated in model studies with TPQ cofactor mimics.[3,4] Although so far unobserved, one must keep in mind that there is always an alternative addition−elimination mechanism (Scheme 1, path B) that can justify the same observed overall stoichiometry. According to the latter mechanism, the active-site base would act on the initially formed carbinolamine that *precedes* the substrate Schiff base. Proton abstraction would result in an aldimine, which would hydrolyze to aldehyde and

Scheme 1

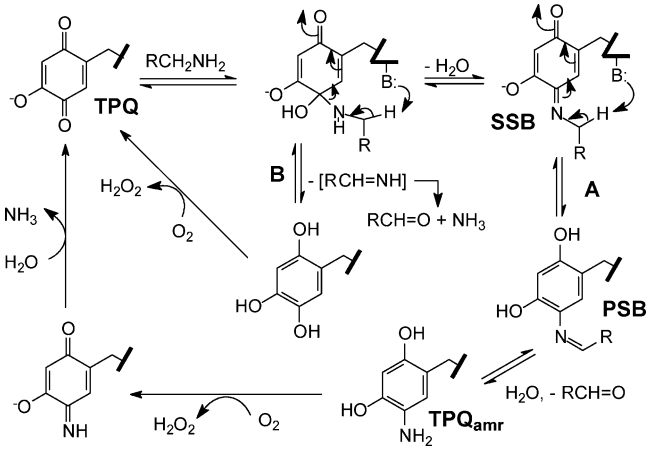

[†] Case Western Reserve University.
[‡] Montana State University.

(1) Brazeau, B. J.; Johnson, B. J.; Wilmot, C. M. *Arch. Biochem. Biophys.* **2004**, *428*, 22−31.
(2) Mure, M.; Mills, S. A.; Klinman, J. P. *Biochemistry* **2002**, *41*, 9269−78.
(3) (a) Wang, F.; Bae, J.-Y.; Jacobson, A. R.; Lee, Y.; Sayre, L. M. *J. Org. Chem.* **1994**, *59*, 2409−2417. (b) Lee, Y.; Sayre, L. M. *J. Am. Chem. Soc.* **1995**, *117*, 3096−3105. (c) Lee, Y.; Sayre, L. M. *J. Am. Chem. Soc.* **1995**, *117*, 11823−11828.
(4) (a) Mure, M.; Klinman, J. P. *J. Am. Chem. Soc.* **1995**, *117*, 8698−8706. (b) Mure, M.; Klinman, J. P. *J. Am. Chem. Soc.* **1995**, *117*, 8707−8718.

10.1021/ja058838f CCC: $33.50

Scheme 2

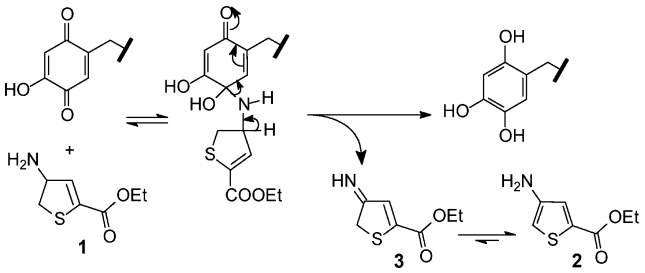

ammonia, and the triol form of the reduced cofactor, which would be reoxidized to quinone. Although this mechanism would result in the same net stoichiometry, it was found that when the enzyme reaction is run anaerobically (single turnover), NH_3 was released only when the enzyme was exposed to oxygen.[5] Since the addition−elimination mechanism would predict that NH_3 and aldehyde should both form following anaerobic single turnover, such observation was the main historic evidence that the enzyme utilizes the transamination mechanism. More recently, various intermediates in the transamination mechanism have been spectroscopically observed.[6−9] Nevertheless, addition−elimination could conceivably be observed for unusual enzyme substrates and is known to be a viable mechanism under certain conditions for the nonenzymatic oxidation of amines by pyrroloquinolinequinone (PQQ) and its analogues,[10,11] as well as for alcohol dehydrogenation by PQQ-dependent alcohol dehydrogenases.[12]

We have been interested in whether a copper amine oxidase might be coaxed to utilize an addition−elimination mechanism for metabolism of an appropriate substrate. We considered as a possible candidate ethyl 4-amino-4,5-dihydrothiophene-2-carboxylate (**1**), where addition−elimination would be followed by a facile tautomerization to the aromatic product ethyl 4-aminothiophene-2-carboxylate (**2**) (Scheme 2). The free carboxylic acid of (*S*)-**1** was previously found to inhibit γ-aminobutyric acid aminotransferase[13] by covalent modification of the pyridoxal 5′-phosphate cofactor, taking advantage of an aromatization step.[14] The zwitterionic free amino acid would be poorly recognized by the copper amine oxidases, but the ethyl ester could be a substrate if the enzyme made an exception to its normally strict preference for unbranched primary amines and accepted this branched primary amine as a substrate.

Preliminary studies on the interaction of **1** with the CAO bovine plasma amine oxidase (BPAO) revealed apparent turnover to give the aromatized product **2** expected from an addition−elimination mechanism. However, in-depth studies described in this paper demonstrate an unprecedented transaminative processing of **1** to yield an aromatized cofactor derivative that would reflect irreversible inactivation were the enzyme not capable of mediating an O_2-dependent oxidation of the cofactor derivative, ultimately releasing **2** as turnover product.

Results

Enantioselective Inhibition of BPAO by 1. Inhibition of BPAO by the *R* and *S* optical antipodes of **1**[13] was followed by the standard benzylamine assay. Two distinct kinetic patterns were observed (Figure 1). The *R* enantiomer displayed a time- and concentration-dependent inhibition of BPAO (Figure 1, left panel), with the level of inhibition plateauing after the first 5−15 min. At the highest concentration examined (640 μM) the maximum inhibition did not quite reach 50%. In contrast, much lower concentrations of (*S*)-**1** were required to inhibit BPAO (Figure 1, right panel), though the time course was biphasic, especially at lower concentrations, where activity decreased in the first 5 min and then recovered more slowly. Nearly 50% inhibition was seen after 5 min of incubation with 5 μM (*S*)-**1**. Since activity is already recovering at this point, we can estimate that there is at least a ∼130-fold difference in $S > R$ inhibitory potency. At higher concentrations of (*S*)-**1** (e.g., 40 μM), the time profile resembled more the behavior for the *R* antipode, though the activity totally recovered after a 24 h dialysis.[15] In fact, enzyme activity recovered to ≥90% following dialysis after long-term incubations with either (*S*)- or (*R*)-**1**, indicating that there is minimal *permanent* covalent modification.

Both (*S*)-1 and (*R*)-1 Are Substrates of BPAO. The recovery of activity of BPAO over time following incubation with **1** demonstrates that it is being metabolized and that it should thus be possible to detect and characterize the enzymatic turnover product. Incubation of **1** (*R*,*S* mixture 63:37) with BPAO in pH 7.2 buffer produced a single ninhydrin- and UV_{365}-positive product, which was characterized as the aromatized amine **2** by thin-layer chromatography (TLC) and HPLC analyses by comparison with an authentic sample prepared from catalytic dehydrogenation of **1**. Control experiments established that no reaction occurred when **1** was incubated in the same buffer solution in the absence of enzyme or in the presence of denatured BPAO, indicating conversion of **1** to **2** is strictly dependent on active enzyme. Compound **2** is the aromatized tautomer of the dehydrogenation product, imine **3** (Scheme 2), that would be generated from an addition−elimination metabolism of **1**. On the other hand, no evidence was found for hydroxythiophene **4**, the aromatized form of the "normal" transamination product **5**, assuming the latter could be hydrolytically released immediately upon tautomerization of substrate Schiff base to product Schiff base.

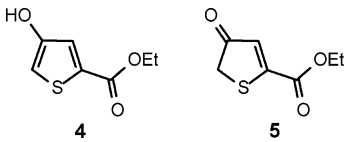

To quantify the metabolism of **1** by BPAO, the reaction progress was monitored by HPLC for the pure *R* and *S*

(5) Janes, S. M.; Klinman, J. P. *Biochemistry* **1991**, *30*, 4599−4605.
(6) Hartmann, C.; Brzovic, P.; Klinman, J. P. *Biochemistry* **1993**, *32*, 2234−41.
(7) Nakamura, N.; Moenne-Loccoz, P.; Tanizawa, K.; Mure, M.; Suzuki, S.; Klinman, J. P.; Sanders-Loehr, J. *Biochemistry* **1997**, *36*, 11479−86.
(8) Medda, R.; Padiglia, A.; Pedersen, J. Z.; Rotilio, G.; Finazzi Agro, A.; Floris, G. *Biochemistry* **1995**, *34*, 16375−81.
(9) Hirota, S.; Iwamoto, T.; Kishishita, S.; Okajima, T.; Yamauchi, O.; Tanizawa, K. *Biochemistry* **2001**, *40*, 15789−96.
(10) (a) Sleath, P. R.; Noar, J. B.; Eberlein, G. A.; Bruice, T. C. *J. Am. Chem. Soc.* **1985**, *107*, 3328−3338. (b) Rodriguez, E. J.; Bruice, T. C. *J. Am. Chem. Soc.* **1989**, *111*, 7947−7956.
(11) (a) Ohshiro, Y.; Itoh, S. *Bioorg. Chem.* **1991**, *19*, 169−189. (b) Itoh, S.; Fukui, Y.; Haranou, S.; Ogino, M.; Komatsu, M.; Ohshiro, Y. *J. Org. Chem.* **1992**, *57*, 4452−4457.
(12) Itoh, S.; Kawakami, H.; Fukuzumi, S. *Biochemistry* **1998**, *37*, 6562−6571.
(13) Adams, J. L.; Chen, T.-M.; Metcalf, B. W. *J. Org. Chem.* **1985**, *50*, 2730−2736.
(14) Fu, M.; Nikolic, P.; Van Breemen, R. B.; Silverman, R. B. *J. Am. Chem. Soc.* **1999**, *121*, 7751−7759.
(15) Long-term incubation (2.5 h) of BPAO with *S*-**1** at the same concentration resulted in ∼10% activity loss that is resistant against dialysis.[16]
(16) Qiao, C. Ph.D. Thesis, Case Western Reserve University, Cleveland, OH, 2004.

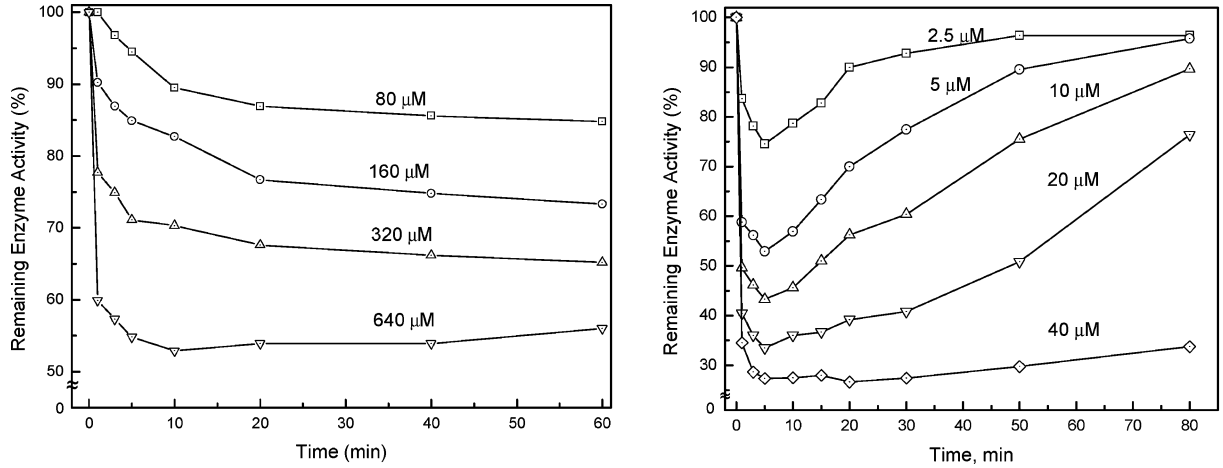

Figure 1. Time-dependent inhibition of BPAO (1.0 μM) by various concentrations of (*R*)-**1** (left) and (*S*)-**1** (right). The enzyme activities represent the slopes of ΔA_{250} for the first 40 s after dilution of the aliquots into 5 mM benzylamine assay solution.

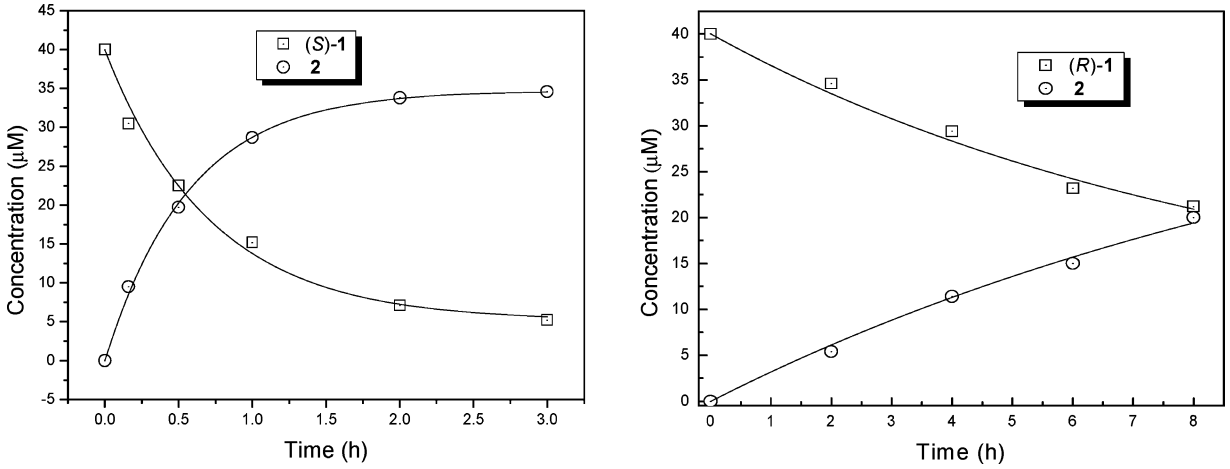

Figure 2. Metabolism of the optically pure enantiomer of **1** (40 μM) by BPAO (0.7 μM). Left panel, (*S*)-**1**; right panel, (*R*)-**1**.

enantiomers, both at 40 μM (Figure 2). The metabolism of **1** to **2** was essentially quantitative for both enantiomers as shown by the nearly 100% material recovery at various time points. The plots of consumption of **1** and formation of **2** over time appeared to be simple exponential curves for both enantiomers. A nonlinear least-squares fit of the product formation curves yielded first-order rate constants (k_1) of 1.8 h^{-1} ($t_{1/2}$ 23 min) for (*S*)-**1** and 0.080 h^{-1} ($t_{1/2}$ 8.7 h) for (*R*)-**1**, respectively. The half-life for metabolism of (*R*)-**1** is 23-fold longer than for (*S*)-**1**. The metabolism of (*S*)-**1** by BPAO was also followed by UV difference spectrophotometry (Figure S1 in Supporting Information). A clean isosbestic conversion of **1** (294 nm) to **2** (250 and 318 nm) was observed, suggesting that any intermediates in the reaction do not accumulate on the steady-state time scale. The slower turnover rate for (*R*)-**1** compared to (*S*)-**1** is consistent with the much slower recovery of enzyme activity when BPAO is incubated with (*R*)-**1** than with (*S*)-**1**, according to the understanding that activity can begin to recover only when most of the inhibitor is metabolized.

The time-dependent stoichiometric conversion of **1** to **2** by BPAO confirmed that both enantiomers of **1** are substrates for BPAO. This result is significant because it shows for the first time not only that a copper amine oxidase can smoothly metabolize a *branched* primary amine but also that metabolism may result in an overall *dehydrogenation* as opposed to the typical *deamination* stoichiometry.

Processing of (*S*)-1 by BPAO Occurs at the Active Site. Mechanistic studies were focused on the more active *S*-enantiomer. At the outset, it was important to first determine whether the initial rapid loss of activity of BPAO upon interaction with (*S*)-**1** (Figure 1, right) was due to its competition with benzylamine for the enzyme active site. The initial rates of oxidative deamination of varying concentrations of benzylamine by BPAO in the presence of varying concentrations of (*S*)-**1** allowed construction of a Lineweaver−Burk plot (Figure 3, left panel), which was found to pass through the same point on the *y*-axis, suggesting that (*S*)-**1** interacts at the enzyme active site as a competitive inhibitor.[17] Moreover, construction of the corresponding Dixon plot (Figure 3, right) allowed estimation of the dissociation constant (K_i) of the complex of BPAO with (*S*)-**1** to be 0.76 μM, suggesting that (*S*)-**1** is a tight binding inhibitor of BPAO.

Anaerobic Reaction of 1 with a TPQ Cofactor Mimic Proceeds According to a Transamination Mechanism. To shed light on the potential enzymatic pathways for metabolism of **1**, we conducted a model reaction of compound **1** with the TPQ cofactor mimic 5-*tert*-butyl-2-hydroxy-1,4-benzoquinone (TBHBQ).[3c,4] A transamination pathway for this reaction (Scheme 3, path A) would lead to a product Schiff base (PSB) that could theoretically hydrolyze but would likely instead

(17) Inhibition of BPAO by compound **1** also met other criteria for a mechanism-based inhibitor; e.g., substrate benzylamine protection.[16]

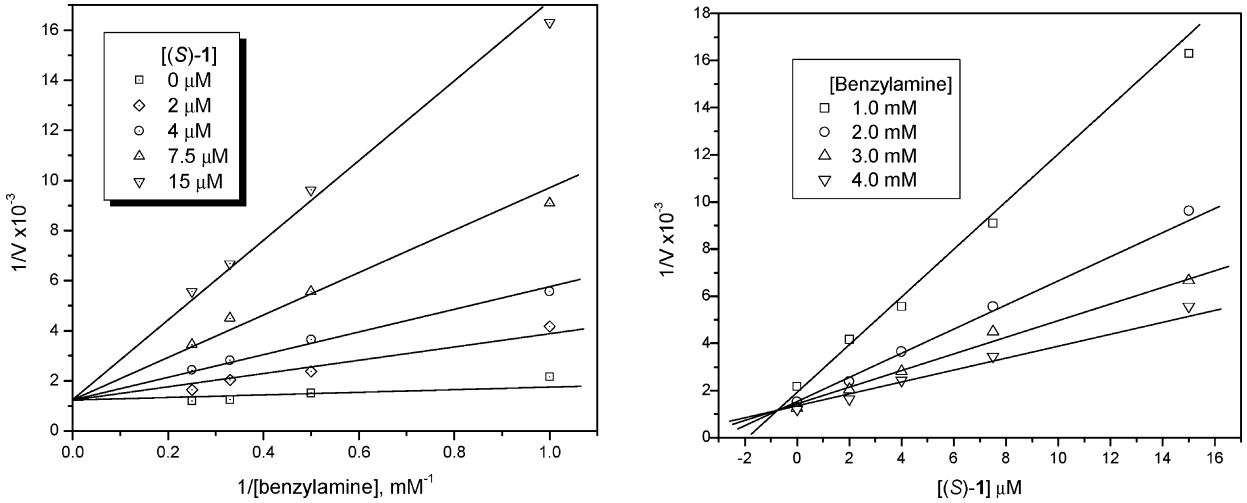

Figure 3. Competitive inhibition of BPAO (1.0 μM) by different concentrations of (*S*)-**1**, pH 7.2, 0.1 M sodium phosphate buffer, 30 °C. Left panel: Lineweaver−Burk plot of enzyme activities (oxidation of benzylamine) measured over the first 40 s following dilution of aliquots of the primary incubation mixture into the assay cuvette. Right panel: Corresponding Dixon plot.

Scheme 3

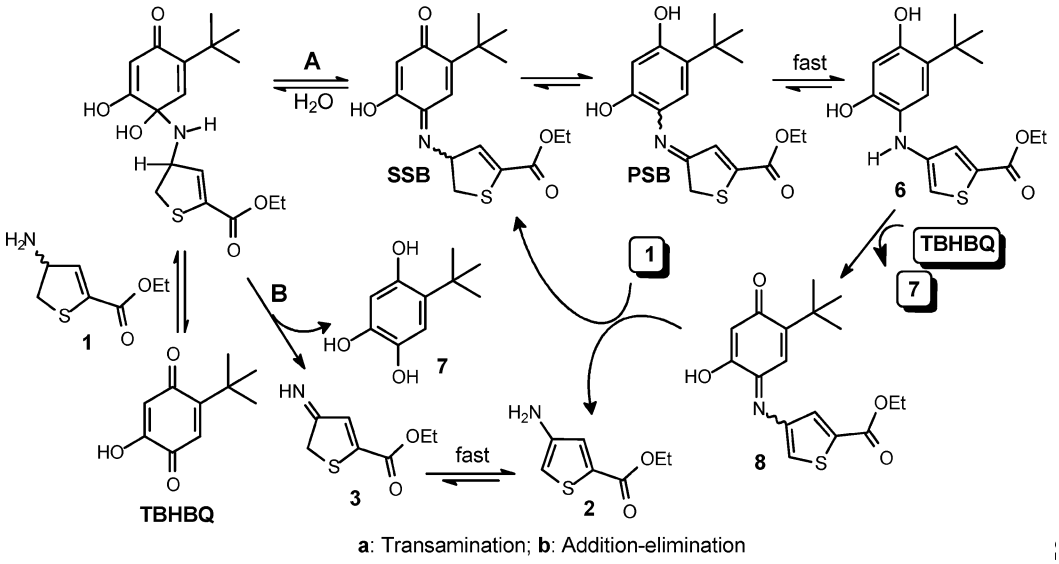

undergo aromatization to give the "coupling product" **6**. In contrast, as discussed above (Scheme 2), the alternative addition−elimination mechanism (Scheme 3, path B) would result in reduction of TBHBQ to the corresponding benzenetriol **7** and imine **3**, which would rapidly tautomerize to **2**.

The model reaction of **1** with TBHBQ was conducted in dimethyl sulfoxide (DMSO) under anaerobic "single turnover" conditions in the presence of excess diisopropylethylamine (DIPEA) as base catalyst,[18] and the initial reaction products were trapped in situ against oxidative evolution by acetylation (with Ac_2O) prior to exposure to air. Three products were isolated and characterized: the acetylated derivative of the aromatization product **2**, the triacetylated derivative of the coupling product **6**, and the triacetylated derivative of benzenetriol **7**. It was found that although **7** is susceptible to autoxidation under the basic reaction conditions, products **2** and **6** are both stable enough to be isolated and characterized directly. The production of *both* **6** and **2** + **7** suggests consideration of the possibility that transamination and addition−elimination reactions, respectively, are operating simultaneously. However, no mechanistic conclusions could be made at this point due to the probable operation of redox interconversions, common to such reactions conducted anaerobically,[3] that can scramble the products. For example, oxidation of **6** by TBHBQ (or the TBHBQ-derived SSB) would generate quinonimine **8**, which could undergo transimination with **1** to give **2**, whereas condensation of **2** with starting TBHBQ and reduction of the resulting quinonimine by triol **7** would give **6**.

The anaerobic reaction of **1** with TBHBQ was also monitored in situ by ^{1}H NMR spectroscopy. Throughout the period of observation (20 h), the only signals observed were starting **1** and products **2**, **6**, and **7**, with the amount of **7** being the same as that of **2**. The relative amounts of **1**, **2**, and **6** were quantified according to their signal integral and plotted over time (Figure 4). The **2**/**6** ratio increased from ∼1:16 at 10 min to ∼1:1.8 at 4 h and then remained nearly constant afterward. Because a typical parallel reaction mechanism would predict a constant ratio of **2** and **6**, the observed apparent lag in generation of **2** is indicative of the *consecutive* reaction **1** → **6** → **2**, with the first

(18) No significant reaction occurred when TBHBQ was incubated with **1** in 0.1 M phosphate buffer, pH 7.2, both aerobically and anaerobically for several days as monitored by UV−vis spectrophotometry.

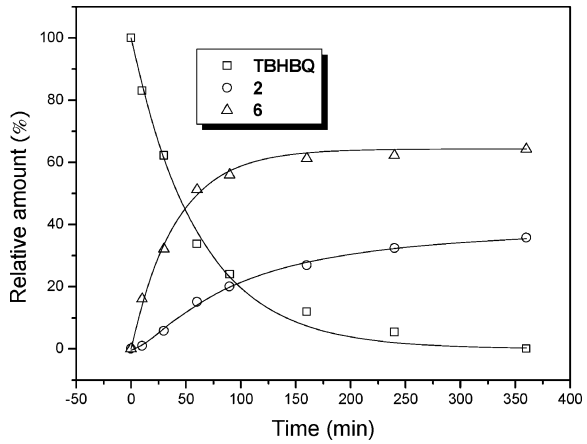

Figure 4. Model reaction of TBHBQ (70 mM) with **1** (70 mM) in the presence of DIPEA (280 mM) in degassed DMSO-d_6 at 25 °C, showing the formation of **2** and **6**. The amounts were quantified by ^{1}H NMR signal integration.

step being faster than the second. This result suggests that the model reaction follows predominantly a transamination mechanism and that apparent addition−elimination product **2** arises from redox cycling evolution of coupling product **6**.

The most likely pathway for conversion of **6** to **2** under the anaerobic model reaction conditions is oxidation of **6** by starting quinone TBHBQ, giving the observed triol **7** and quinonimine **8**, which would undergo transimination with starting amine **1** to give **2** (thereby regenerating the substrate Schiff base). A control NMR tube experiment to ascertain whether TBHBQ could oxidize **6** in DMSO/DIPEA surprisingly revealed no significant reaction under argon, but reaction quickly ensued upon admission of air. However, other control experiments showed that, in the DMSO/DIPEA condition, **7** but not **6** undergoes air oxidation. We thus propose that the redox interchange TBHBQ + **6** ⇌ **7** + **8** represents an unfavorable equilibrium, which is pulled to the right in air by O_2-dependent oxidation of **7** to TBHBQ. When the model reaction is run anaerobically, we propose that the equilibrium is pulled to the right by the removal of **8** in reacting with **1**.[19] This would suggest that conversion of **6** to **2** would cease once starting **1** is consumed. This conclusion is consistent with the results shown in Figure 4, where despite our claim of operation of the consecutive reaction **1** → **6** → **2**, no further conversion of **6** to **2** occurs once **1** has been depleted (at 300−350 min).

Assuming that conversion of **6** to **2** occurs according to shifting of an unfavorable redox cycling equilibrium that is not directly observable, we sought conclusive evidence for such where the fate of **8** could be independently traced through a labeling strategy, using different alcohol esters (e.g., methyl vs ethyl esters). These experiments, following the anaerobic reaction of TBHBQ with **1** carrying one ester label in the presence of added **6** or **2** carrying a second ester label (Supporting Information), clearly demonstrated the ability of **6** to be converted to **2**, *but not vice versa*, during anaerobic turnover of TBHBQ with **1**. At the same time, we could find no evidence for the ability of **2** to undergo condensation with TBHBQ, which would be required for redox cycling conversion of **2** to **6**, thus ruling out the ability of the addition−elimination reaction to rationalize generation of **6** in the model reaction. The unreactivity of **2** is not surprising, considering that it is isoelectronic with an aniline whose nucleophilicity is further reduced by resonance delocalization of the nitrogen lone pair onto the carbethoxy substituent. All these results support the interpretation that generation of **2** in the model reaction results strictly as a consequence of the transamination mechanism according to Scheme 3, path A.

Conversion of TBHBQ-Derived Coupling Product 6 to 2 under Aerobic Conditions. If transamination (Scheme 3, path A) represents the mechanism by which the enzyme processes the conversion of **1** to **2**, one can postulate that formation of the coupling product (like **6**) reflects modification of the TPQ cofactor that rationalizes the initial quick inactivation of BPAO by **1** and that the recovery of activity then reflects oxidation to the quinonimine (like **8**) and subsequent dissociation or transimination of the latter. However, unlike the model system described above, where oxidation of **6** was effected by the excess starting quinone available (Scheme 3), oxidation of the coupling product in the enzyme case would have to be effected by dioxygen. It was thus important to explore the chemical behavior of **6** under various aerobic reaction conditions.

In contrast to the inertness of **6** in anhydrous DMSO, aerobic incubation of **6** in 50% buffered (pH 7.2) aqueous DMSO exhibited a slow but clean *consecutive* reaction as monitored spectrophotometrically (Figure 5). A species absorbing at 290 and 420 nm was observed to form as intermediate, and TBHBQ (∼500 nm) and **2** (∼320 nm) were the final products (spectra of the various model compounds are given in Figure S4 in Supporting Information). The formation of TBHBQ and **2** was confirmed by comparative TLC with authentic samples, whereas the intermediate was characterized as quinonimine **8**, which could be isolated in fair yield (55%) from autoxidation of **6** in 1:4 buffer/CH_3CN. The spectral change at 490 nm (the isosbestic point between **8** and TBHBQ) in the first 3 h, and the spectral change at 420 nm after 4 h, both appeared to be exponential, thereby permitting the estimation of the pseudo-first-order rate constants for autoxidation (0.473 h^{-1}, $t_{1/2}$ 1.5 h) and hydrolysis (0.126 h^{-1}, $t_{1/2}$ 5.5 h), respectively (eq 1). The hydrolysis step

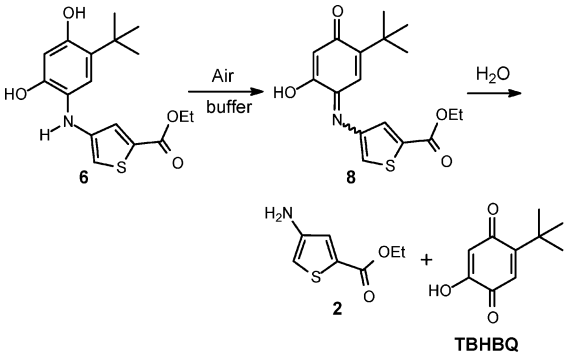

(1)

is 3.7-fold slower than autoxidation and is thus rate-limiting. Essentially the same rate constant for the hydrolysis step was obtained starting alternatively from authentic **8** under the same conditions (data not shown). Addition of 0.1 mM diethylenetriaminepentaacetic acid (DTPA) into the same reaction did not alter the rates for either step. This may suggest that the observed oxidation and hydrolysis proceeds without the obligatory need for trace transition metal catalysis.

(19) We cannot rule out the possibility that oxidation of **6** to **8** is mediated by the TBHBQ/**1**-derived SSB, where the reduced SSB would then be reoxidized by TBHBQ.

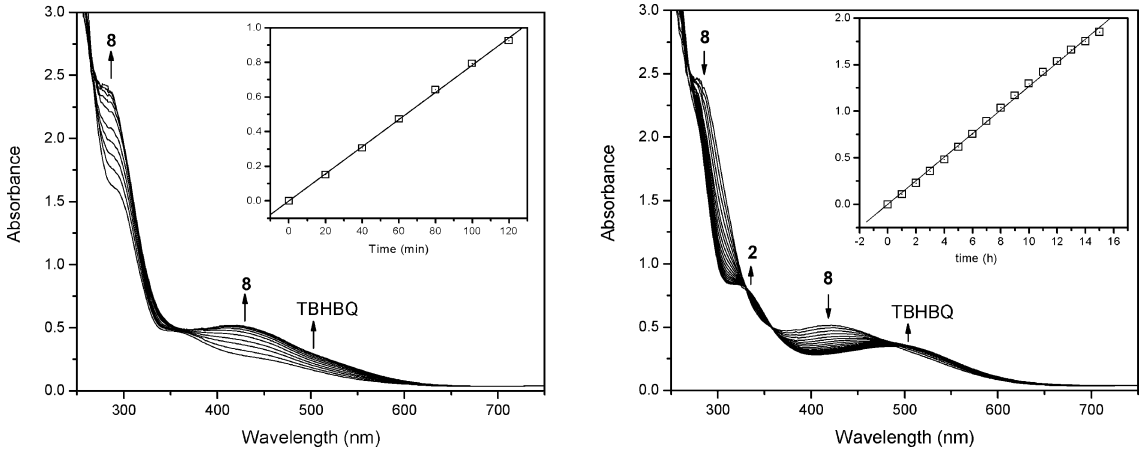

Figure 5. Aerobic incubation of **6** (0.15 mM) in 1:1 DMSO and 0.05 M HEPES buffer, pH 7.2, at 25 °C, showing autoxidation to quinonimine **8** in the early stage (the first 3 h, left panel, 20 min time intervals), and subsequent hydrolysis of **8** to form TBHBQ and **2** in the later stage (4−22 h, right panel, 1 h time intervals). Insets: Pseudo-first-order ln $[(A_\infty - A_0)/(A_\infty - A_t)]$ vs t plots obtained from ΔA_{490} for autoxidation and ΔA_{420} for hydrolysis, respectively.

Chart 1

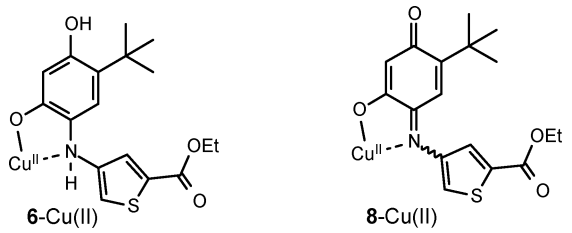

Nonetheless, the presence of Cu(II) at the active site of CAOs and its role in the oxidative half-reaction of substrate turnover,[20−23] prompted us to examine the effect of Cu(II) on the above autoxidation−hydrolysis chemistry. When the same incubation of **6** (buffered aqueous DMSO) was conducted in the presence of 1 mol equiv of Cu(II), the solution *rapidly* (within 30 s) turned reddish-yellow (283, 390, and 500 nm), which then persisted without further spectral change for 2 days. At this point, if the resulting solution was treated with excess DTPA (0.3 mM) to chelate the Cu(II), it quickly turned yellow with the appearance of the characteristic chromophores for **8** (290 and 420 nm; see Figure S2 in Supporting Information), which then underwent slow hydrolysis to give TBHBQ and **2**. An independent control with authentic **8** established that the initially formed reddish-yellow solution was actually the complex **8**−Cu(II) (Chart 1), which is stabilized against hydrolysis, probably on account of forming a five-membered ring chelate. The pseudo-first-order rate constant (k_1) for the Cu(II)-mediated autoxidation of **6** was measured as 0.101 s^{-1} ($t_{1/2}$ 7 s) by monitoring ΔA_{390} over time (Figure S3 in Supporting Information), showing a ∼770-fold rate enhancement compared to the reaction without added Cu(II). This significant promotion by Cu(II) likely reflects its initial coordination to **6** (Chart 1) and then rapid reaction of the activated **6**−Cu(II) with O_2. In the enzyme case, although chelation of the coupling product to Cu(II) in the manner permitted in the model study in solution would likely be precluded, any type of interaction with the Cu(II) is expected to facilitate the autoxidation process.

Scheme 4

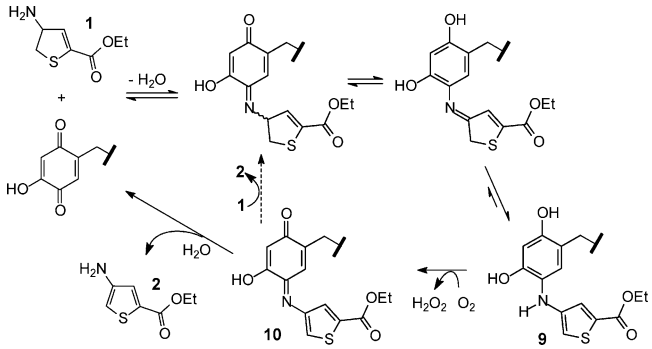

Mechanism of BPAO-Mediated Metabolism of (*S*)-1: (i) Kinetics of Aerobic Activity Recovery following Anaerobic Inhibition by (*S*)-1. The studies described above demonstrate that the conversion of **1** to **2** in the model reaction with TBHBQ follows a transamination−oxidation pathway. Nonetheless, whether the enzyme uses transamination or addition−elimination must be independently established. Transamination (Scheme 4) predicts that **2** would form only upon aerobic reoxidation of the coupling product **9** generated at the end of anaerobic single turnover. Addition−elimination predicts that turnover product **2** should be present at the end of anaerobic single turnover along with the benzenetriol form of the reduced TPQ cofactor. In a previous study on the interaction of BPAO with simple alkylhydrazines,[24] we concluded that the benzenetriol form of the cofactor is generated anaerobically but is reoxidized immediately upon aliquoting into the aerobic benzylamine oxidase activity assay, so that the measured activity is thus indistinguishable from the control. In the present study, using $NaBH_4$ to directly generate the benzenetriol TPQ form (see Supporting Information), we verified that the latter reoxidizes immediately in the aerobic activity assay, and thus, any addition−elimination process generating the benzenetriol would *not* be detectable by the standard activity assay. On the other hand, if the transamination mechanism were followed, resulting in the coupling product **9** (Scheme 4), recovery of enzyme activity would

(20) Dooley, D. M.; McGuirl, M. A.; Brown, D. E.; Turowski, P. N.; McIntire, W. S.; Knowles, P. F. *Nature* **1991**, *349*, 262−4.
(21) Hirota, S.; Iwamoto, T.; Kishishita, S.; Okajima, T.; Yamauchi, O.; Tanizawa, K. *Biochemistry* **2001**, *40*, 15789−96.
(22) Mills, S. A.; Goto, Y.; Su, Q.; Plastino, J.; Klinman, J. P. *Biochemistry* **2002**, *41*, 10577−84.
(23) Kishishita, S.; Okajima, T.; Kim, M.; Yamaguchi, H.; Hirota, S.; Suzuki, S.; Kuroda, S.; Tanizawa, K.; Mure, M. *J. Am. Chem. Soc.* **2003**, *125*, 1041−55.
(24) Lee, Y.; Jeon, H. B.; Huang, H.; Sayre, L. M. *J. Org. Chem.* **2001**, *66*, 1925−1937.

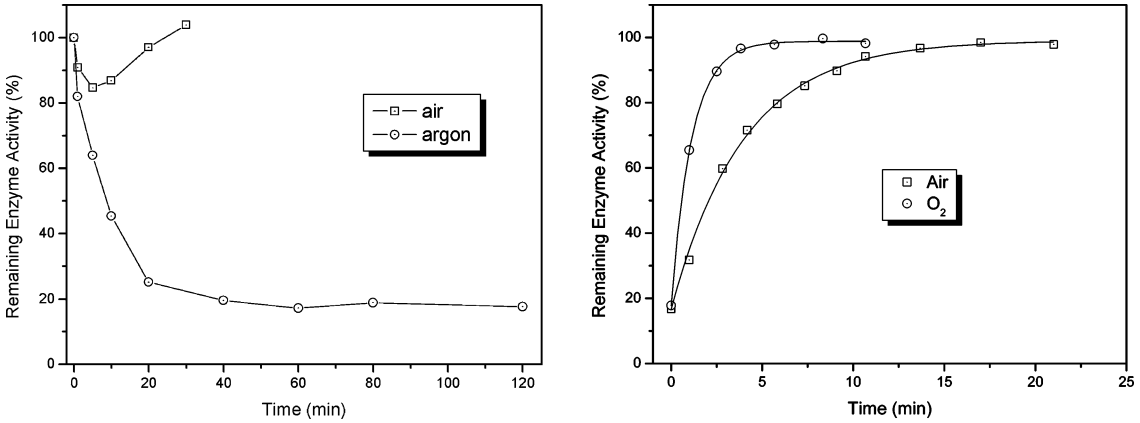

Figure 6. Left panel: Time-dependent activity changes of BPAO (1.0 μM) upon incubation with (*S*)-**1** (1.2 μM) in 0.1 M phosphate buffer, pH 7.2, at 30 °C under aerobic and anaerobic conditions. Right panel: time-dependent recovery of activity upon 10 s of bubbling with air or O_2 of BPAO (1.0 μM) that was anaerobically inhibited by incubation with (*S*)-**1** (1.2 μM) for 60 min. Enzyme activity represents ΔA_{250} over the first 40 s upon dilution into the air-equilibrated benzylamine assay mixture.

Table 1. Kinetic Parameters for O_2-Dependent Activity Recovery of BPAO Anaerobically Inactivated by (*S*)-**1**[a]

atmosphere	k_1 (min^{-1})	$t_{1/2}$ (min)	Act$_\infty$ (%)
air	0.25 ± 0.01	2.77	99.1 ± 0.8
O_2	0.88 ± 0.02	0.79	98.8 ± 0.3

[a] The inactivated enzyme samples were generated by incubating BPAO (1.0 μM) with (*S*)-**1** (1.2 μM) in 0.1 M phosphate buffer, pH 7.2, under argon at 30 °C for 60 min and then bubbled with either air or O_2 for 10 s.

require the oxidative formation and subsequent hydrolysis of quinonimine **10** (Scheme 4), which, on the basis of our model studies, would not be instantaneous. On the basis of these scenarios, the mechanism used by the enzyme could be theoretically distinguished by any one of three different approaches: (i) determining the kinetics of aerobic recovery of anaerobically inhibited enzyme, (ii) determining whether **2** is present after anaerobic single turnover or forms only upon aerobic reoxidation, and/or (iii) determining the fate of the cofactor upon anaerobic single turnover by spectroscopic means.

According to the first approach, the activity of BPAO during incubation with a slight excess of (*S*)-**1** under aerobic and anaerobic conditions was monitored over time by the standard aliquot method (10-fold dilution into buffered benzylamine and measurement of the slope for benzaldehyde formation over the first 40 s). In the aerobic reaction (Figure 6, left panel), the enzyme activity dipped a bit (to a minimum of 83%) at 5 min and then fully recovered within 30 min. When the same incubation was conducted under argon, the enzyme activity decreased all the way down to ~20% in 20 min and then remained constant within the time frame of observation (2 h). However, bubbling of the anaerobic incubation solution with air or O_2 after 1 h resulted in a time-dependent recovery of enzyme activity (Figure 6, right panel). The recovery of enzyme activity upon exposure to air or O_2 appeared to be exponential and could be analyzed by pseudo-first-order nonlinear least-squares fits. Values of the calculated rate constants (k_1), half-lives ($t_{1/2}$), and final enzyme activities at long reaction time (Act$_\infty$) are listed in Table 1. The half-life for air bubbling is 3.5 times longer than the one for O_2 bubbling.

The noninstantaneous O_2-dependent recovery of enzyme activity upon sampling of the anaerobic incubation reaction supports a transamination mechanism for the processing of (*S*)-**1** by BPAO and is inconsistent with the presence at this time of the benzenetriol form of the reduced TPQ cofactor predicted by addition−elimination. The only caveat would be if the enzyme uses addition−elimination and the presence of product **2** bound to the enzyme somehow slowed the otherwise instantaneous O_2-dependent oxidation of the benzenetriol form of the TPQ cofactor. An independent experiment established that incubation of both native and borohydride-reduced BPAO with 1 equiv of **2** did not result in a detectable diminution of enzyme activity as measured by the benzylamine assay (Supporting Information). We conclude that the kinetics of the interaction of BPAO with (*S*)-**1** in Figure 6 represents a transamination reaction pathway. The time-dependent anaerobic inactivation indicates formation of the "coupling product" **9**, whereas the aerobic enzyme activity recovery reflects regeneration of the TPQ cofactor through the oxidation−hydrolysis pathway via quinonimine **10** (Chart 1). The fact that the enzyme activity recovery upon O_2 bubbling is 3.5 times faster than upon air bubbling (Table 1) suggests that *oxidation of the coupling product cofactor is at least partially rate-limiting in the oxidative half-reaction*.

It should be pointed out that the activity of BPAO incubated with at least a slight excess of (*S*)-**1** never reached *zero* even under anaerobic conditions (Figure 6) or with a large excess of (*S*)-**1** (Figure 1). There are two possible explanations for observation of this 20−30% residual activity: (i) according to the transamination reaction, it may represent oxidation of the coupling product **9** that occurs within the aerobic *dead time* of the benzylamine assay (40 s), or (ii) it may represent a partial contribution by an addition−elimination reaction, where 20−30% of the TPQ cofactor is present in its benzenetriol reduced form at the end of anaerobic single turnover.

(ii) HPLC Analysis of Anaerobically Inactivated BPAO. The second approach was to determine if there is any significant release of turnover product **2** during anaerobic incubation of BPAO with (*S*)-**1** due to a possible contributing addition−elimination pathway. Thus, BPAO (100 μM) was incubated with 1 equiv of (*S*)-**1** (100 μM) under argon for 30 min and then precipitated with trichloroacetic acid (TCA) under argon. The supernatant was withdrawn and subjected to HPLC analysis, showing a complete absence of (*S*)-**1** and the presence of a small amount of **2** that corresponded to 2% of starting (*S*)-**1**. When the same incubation was conducted under strictly anaerobic

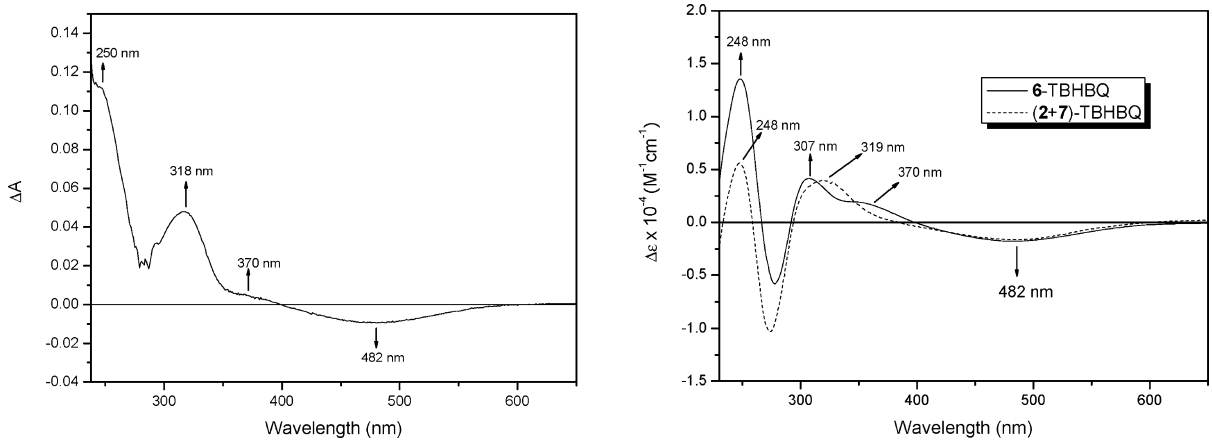

Figure 7. Left panel: UV−vis difference spectrum (against native BPAO) obtained from anaerobic reaction of BPAO (80 μM) with (*S*)-**1** (100 μM) in 0.1 M phosphate buffer, pH 7.2, at 25 °C. Right panel: UV−vis difference spectra between **6** and TBHBQ, and between (**2** + **7**) and TBHBQ. All the original spectra are shown in Supporting Information (Figures S4 and S5).

conditions (added glucose/glucose oxidase/catalase under argon), only 0.7% **2** was detected. The caveat for interpreting this result, however, is that the actual amount of **2** generated in the reaction could have been underestimated due to adsorption to the protein during TCA precipitation. A control experiment where the anaerobic incubation mixture was exposed to air for 60 min to ensure complete turnover and release of **2** prior to precipitation, indeed revealed only a 65% accountable "recovery" of **2**. The recovery did not improve when the same protein sample was first denatured anaerobically with guanidine/β-mercaptoethanol and then worked up by the same procedure. Other control experiments, (i) omitting the initial anaerobic period and (ii) incubating 1.2 equiv of **2** with the native enzyme, resulted in a similar loss of 35−40% **2** following precipitation of the protein. As expected, greater losses of **2** were observed when using lower concentrations of (*S*)-**1** relative to enzyme. Despite the partial unaccountability of **2** due to apparent absorption to the protein, the finding that only trace levels of **2** are detected upon analysis of the anaerobic incubation is inconsistent with a significant contribution by the addition−elimination reaction. This suggests that the residual 20−30% enzyme activity seen upon sampling the preparation of BPAO anaerobically inhibited by (*S*)-**1** (Figure 6) represents aerobic recovery of enzyme activity during the 40 s benzylamine assay. This conclusion is consistent with the measured half-life of activity recovery (Table 1).

(iii) UV−Vis Spectrophotometric Studies on the Reaction of BPAO with (*S*)-1. The third approach to determining enzyme mechanism was to spectroscopically observe the TPQ-derived intermediates following anaerobic single turnover. Addition of degassed (*S*)-**1** (100 μM) to an anaerobic solution of BPAO (80 μM) in 0.1 M phosphate buffer, pH 7.2, immediately caused bleaching of the TPQ chromophore at 482 nm and the appearance of several new peaks, as clarified by the difference spectra against the native BPAO (Figure 7, left panel). No further spectral changes were detected over time following the initial rapid reductive half-reaction. Exactly the same difference spectrum was obtained when the reaction was conducted in strictly anaerobic conditions (glucose/glucose oxidase/catalase/argon).

To help interpret the initial spectral change, reference difference spectra were generated from the TBHBQ-derived model species for either the transamination outcome (TBHBQ vs **6**) or the addition−elimination outcome (TBHBQ vs **2** + **7**).[25] The key spectral difference between these two outcomes (Figure 7, right panel) lies in the range of 300−400 nm, with transamination featuring a peak at 307 nm and a shoulder at ∼370 nm, whereas addition−elimination features only a broad band at 319 nm. The difference spectrum for the enzyme case did not exactly match either of the two model difference spectra: the ∼370 nm shoulder peak matches the same feature in the model difference spectrum for transamination, but the 318 nm peak appears consistent with the model difference spectrum for addition−elimination. We considered the possibility that the enzyme spectrum may reflect a conformational rearrangement in the active site, permitting interaction with the copper, but the presence of Cu(II) did not significantly alter either model difference spectrum. The finding that the longest wavelength peaks for the model compounds are at ∼319 nm for **2** + **7** and ∼370 nm for **6** likely reflects red-shifting of the n → π* transition due to the extended π conjugation present in **6** (when planar in solution) that is not present in **2** + **7**. We suggest that conformational constraints in the enzyme active site may cause the 307 nm band in **6** to shift to 318 nm, which just happens to coincide with the lowest energy transition in **2**. In the case of possible conformational restrictions, one cannot expect an exact correspondence between reference model compound spectra and the spectroscopic behavior of the enzyme reaction.

When the above anaerobically inactivated BPAO was exposed to O_2, time-dependent spectral changes were observed (Figure S6 in Supporting Information). The major event at short time (first 20 min) was the appearance and growth of two peaks at 320 and 250 nm (Figure S7 in Supporting Information), indicating the generation of some **2**, but there were no spectral changes observed in the visible region indicative of a change in status of the cofactor. Indeed, the benzylamine assay showed that the enzyme was still mainly inhibited at this point (27% activity). This "lag" results from the need to metabolize the 20 μM excess of (*S*)-**1** and the sluggish reoxygenation of the concentrated enzyme solution under the conditions of simple O_2 exposure (diffusion-limited).

At longer times, however, dramatic spectral changes were observed (Figure 8). First, the constant decrease at 250 nm right

(25) We considered correcting these difference spectra for the fact that (*S*)-**1** was in excess (by 25%) over the enzyme. However, because of the weak relative extinction coefficient of **1**, there was only minor alteration of the difference spectra near 290 nm, a noncritical region of interpretation.

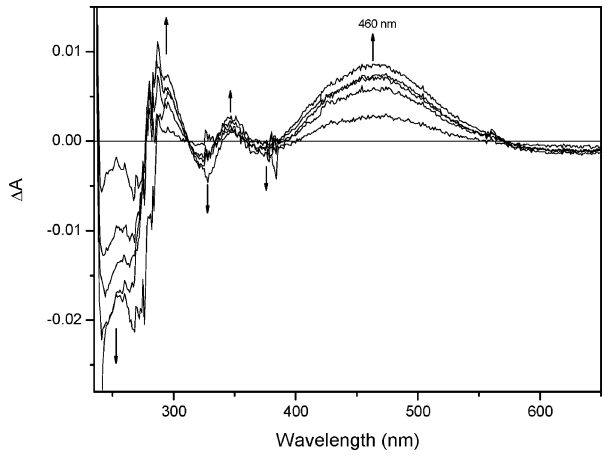

Figure 8. Time-dependent (10 min interval) UV−vis difference spectra recorded after O_2 exposure for 20 min of BPAO (80 μM) anaerobically inactivated with (*S*)-**1** (100 μM). The spectra were generated against the spectrum at the 20 min time point.

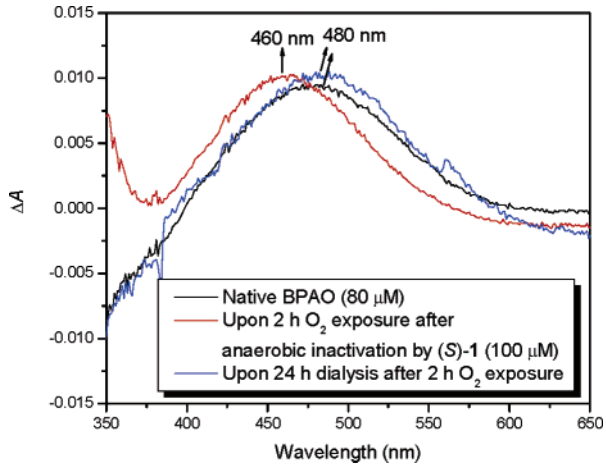

Figure 9. UV−vis difference spectra (against the anaerobically (*S*)-**1**-inactivated BPAO) of native BPAO, of anaerobically (*S*)-**1**-inactivated BPAO after 2 h of O_2, and of the latter mixture after dialysis against 0.1 M phosphate buffer, pH 7.2, for 24 h. The original spectra are shown in Figure S8 in Supporting Information.

after complete turnover of the *excess* (*S*)-**1** at the 20 min time point is consistent with conversion of coupling product **9** to turnover product **2**, since although the model coupling product **6** and **2** both absorb at 250 nm, the extinction coefficient for **6** is higher (Figure S4 in Supporting Information). The most evident spectral change, however, was the appearance and growth of a new peak at 460 nm (the enzyme solution gradually turned reddish yellow), which maximized after 70 min (Figure 8), and then persisted at least for 48 h. The benzylamine assay showed that the enzyme activity had fully recovered at this stage. Upon dialysis against 0.1 M phosphate buffer, pH 7.2, for 24 h, the 460 nm chromophore readily shifted to the TPQ chromophore at 482 nm (individual spectra are shown in Figure S8, Supporting Information, and the difference spectra in Figure 9), with full preservation of the enzyme activity. Interestingly, an aerobic titration of native BPAO with **2** recapitulated the reddish-yellow color and the same 460 nm spectroscopic signature (Figure S9 in Supporting Information), with full activity being retained according to the benzylamine assay. These latter observations suggest that the 460 nm chromophore represents either quinonimine **10** or a high-affinity noncovalent enzyme product complex (that perturbs the TPQ chromophore), either of which is in equilibrium with native BPAO and free **2**.

To address the nature of the 460 nm species, we first asked the question of what other types of molecules might cause the same spectral shift. Aniline, but not its *N*-methyl or *N*,*N*-dimethyl derivatives, was able to reproduce the blue shift of the TPQ chromophore. Of course, the lack of reaction of the latter two could represent a steric effect rather than their inability to form a Schiff base. Nonetheless, if the unique behavior of aniline reflected its ability to form the TPQ Schiff base, borohydride reductive quenching of the complex should lead to a catalytically inactive anilinoresorcinol form of the cofactor (oxidation and hydrolysis, if it occurred, would at least be noninstantaneous), as occurs with substrate benzylamine.[26] However, under the same conditions where borohydride reduction of the native enzyme resulted in an immediate total quench of the TPQ chromophore, yet rapid assay displayed full activity (see Supporting Information), $NaBH_4$ treatment of the BPAO−aniline complex only partially quenched the 420 nm chromophore, and there was no reduction in activity upon immediate enzyme assay (data not shown). The independently generated BPAO−**2** complex behaved the same way. Although one possible explanation is that the arylamines are forming a noncovalent complex in a manner that blocks borohydride access to the TPQ, further studies will be required to define the nature of the 460 nm chromophore. Comparison of the difference spectrum in Figure 8 to appropriate model compound difference spectra was also inconclusive (Supporting Information).

Discussion

Enantioselectivity in the Processing of 1. The copper-containing quinone-dependent amine oxidases have been historically described as an enzyme class capable of conversion of unbranched primary amines to aldehydes. Since chiral, branched amines such as α-methylbenzylamine are then nonsubstrates, there has been little information on possible enantioselective metabolism by these enzymes. Recently, two nonmammalian quinoenzymes were reported to be capable of metabolizing the branched primary amine amphetamine,[27] though substrate activity was poor and identification of the ketone product was not described. It has been presumed that the usual failure of TPQ-dependent amine oxidases to process α-branched primary amines to ketones is one of steric unacceptance. The constrained bond angles of the five-membered ring confer a steric advantage to **1**, possibly explaining its ability to be readily processed by BPAO, though it must be appreciated that complete metabolism represents recovery from a mechanism-based inactivation event.

The high degree of enantioselectivity for metabolic production of the final turnover product **2** from (*S*)-**1** (Figure 2) seems to be related to the different inhibitory behavior between the *R* and *S* isomers shown in Figure 1. Theoretically, enantiodiscrimination in the processing of **1** can occur at one or more of the three steps implicated in the overall reaction prior to stereoconvergence between processing of the two enantiomers: (1) initial binding and formation of the carbinolamine generated from nucleophilic attack at the TPQ C5 carbonyl, (2) dehydration of the carbinolamine to give the SSB, and (3)

(26) Hartmann, C.; Klinman, J. P. *J. Biol. Chem.* **1987**, *262*, 962−965.
(27) Hacisalihoglu, A.; Jongejan, A.; Jongejan, J. A.; Duine, J. A. *J. Mol. Catal. B. Enzymol.* **2000**, *11*, 81−88.

Chart 2

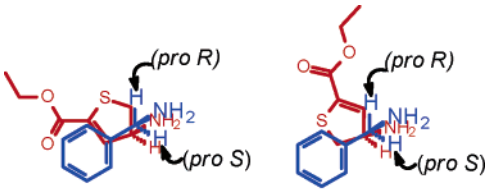

(*S*)-**1**: favorable (*R*)-**1**: unfavorable

tautomerization of SSB to PSB mediated by the active-site catalytic base. The latter step has been the key focus of previous studies to determine possible stereospecific α-deprotonation of normal prochiral primary amine substrates.[28] α-Deprotonation was shown to be nonstereospecific in the cases of BPAO metabolism of dopamine and tyramine,[29−31] suggestive of the possibility for "mirror image" binding of these substrates with respect to the catalytic base. In the case of BPAO metabolism of benzylamine, both nonstereospecific[32] and *pro-S*-specific[33] α-deprotonation have been reported. If one considers a preferred abstraction of the *pro-S* α-proton for bound benzylamine as the reference (the benzylamine *pro-S* and *pro-R* positions are labeled in Chart 2), **1** can be superimposed on the benzylamine molecule to align the two amino groups and to align the phenyl ring of benzylamine with the π portion of inhibitor **1** (4,5 C═C and carboxyl). When this is done (Chart 2, left panel), the available α-proton of the superimposed (*S*)-**1** coincides with the *pro-S* α-proton of benzylamine. Assuming the latter overlap represents the preferred orientation for binding to BPAO, active-site base-mediated removal of the α-proton for (*R*)-**1** would require accommodation of a different spatial orientation of the molecule (Chart 2, right panel), which we propose to be unfavorable.

Mechanism. At the outset, the apparent dehydrogenation process whereby **1** is metabolized to **2** by BPAO suggested consideration of an addition−elimination mechanism. However, we have demonstrated that transamination is the only pathway involved in both the model and the enzyme reactions. In the model case, the apparent addition−elimination products **2** and **7** formed in the anaerobic reaction of **1** with TBHBQ were shown to arise from the primary transamination product **6** via a redox-cycling process as evidenced by the ester-labeling experiments (Supporting Information). In the enzyme case, involvement of transamination as the only pathway was confirmed by kinetic studies on enzyme reactivation and HPLC analysis of the reaction mixture following anaerobic incubation of the enzyme with (*S*)-**1**. The observed net dehydrogenation (as opposed to the typical deamination) results from an unprecedented pathway where the product Schiff base tautomerizes to an aromatic "coupling product" derivative of the TPQ cofactor, thereby averting the normal product Schiff base hydrolysis, but which can still ultimately undergo oxidation to a quinonimine intermediate that releases the apparent dehydrogenation product **2** upon hydrolysis (or transimination with starting **1**).

Because both transamination and addition−elimination pathways require active-site base-mediated removal of the same substrate α-proton, the lack of observation of addition−elimination for the TPQ-dependent enzymes is not likely to reflect orientation issues. Instead, the preference for transamination in both model and enzyme reactions probably reflects the short lifetime of the carbinolamine intermediate that precedes the substrate Schiff base. A detailed study of the mechanism of amine oxidation by PQQ analogues revealed that transamination predominates below pH 10, though addition−elimination competes at higher pH where dehydration of the carbinolamine is slowed.[10b] Although so far still unobserved, the appearance of an addition−elimination pathway for the TPQ-dependent amine oxidases might still transpire if structural features in the enzyme and/or substrate lengthen the lifetime of the carbinolamine intermediate by slowing its dehydration to the SSB. At the same time, the observation of transamination in the present study may indicate that TPQ is more intrinsically disposed toward this mechanism than is PQQ.

Role of Cu(II) in the Oxidative Half-Reaction. Regardless of whether the 460 nm species generated at the end of O_2-dependent reactivation of anaerobically **1**-inactivated BPAO represents quinonimine **10** or a BPAO−**2** noncovalent complex, the finding that enzyme activity at this stage is indistinguishable from the control shows that conversion of this enzyme form to substrate Schiff base in the presence of substrate (e.g., benzylamine) is rapid relative to its O_2-dependent generation from **9**. *A conclusion that oxidation of* **9** *is the rate-limiting step of the oxidative half-reaction would be consistent with the observed dependence on* O_2 (O_2 > *air) of the recovery of enzyme activity* (Table 1).

What factors control the mechanism of oxidation of coupling product **9**, relative to the normal oxidation half-reaction of the enzyme? In this regard, it is interesting to compare the kinetic patterns between the model and enzyme cases. In the model reaction, whereas transition metal-free autoxidation of coupling product **6** is relatively slow ($t_{1/2}$ 1.5 h), the presence of 1 mol equiv of Cu(II) accelerates the autoxidation of **6** by a factor of 770 ($t_{1/2}$ 7 s). In comparison, aerobic oxidation of **9** in the enzyme has a $t_{1/2}$ of 2.8 min (Table 1), nearly the logarithmic average between the two model system results. Transition metal ions are well-known to be capable of catalyzing autoxidation reactions via coordination to an autoxidizable substrate and activation of the latter toward reaction with O_2. Because it is hard to imagine how other active-site residues would promote an autoxidation reaction, the intermediate rate in the enzyme case suggests that the active-site Cu(II) is promoting the oxidation of **9**, but not to the extent that would be expected if **9** could coordinate directly to the active-site Cu(II). At least in the native copper-containing amine oxidases, when TPQ is in the active conformation, the active-site Cu(II) only indirectly interacts with the TPQ cofactor (at best through a water molecule to the C2 oxygen),[1,34,35] as opposed to the chelating coordination possible in the model system between Cu(II) and the C4 oxygen and C5 nitrogen of **6** (Chart 1). We propose that the nearby

(28) Coleman, A. A.; Scaman, C. H.; Kang, Y. J.; Palcic, M. M. *J. Biol. Chem.* **1991**, *266*, 6795−800.
(29) Summers, M. C.; Markovic, R.; Klinman, J. P. *Biochemistry* **1979**, *18*, 1969−79.
(30) Yu, P. H. *Biochem. Cell. Biol.* **1988**, *66*, 853−61.
(31) Coleman, A. A.; Hindsgaul, O.; Palcic, M. M. *J. Biol. Chem.* **1989**, *264*, 19500−5.
(32) Yu, P. H.; Davis, B. A. *Int. J. Biochem.* **1988**, *20*, 1197−201.
(33) Battersby, A. R.; Staunton, J.; Klinman, J. P.; Summers, M. C. *FEBS Lett.* **1979**, *99*, 297−298.
(34) Mills, S. A.; Goto, Y.; Su, Q.; Plastino, J.; Klinman, J. P. *Biochemistry* **2002**, *41*, 10577−84.
(35) Kishishita, S.; Okajima, T.; Kim, M.; Yamaguchi, H.; Hirota, S.; Suzuki, S.; Kuroda, S.; Tanizawa, K.; Mure, M. *J. Am. Chem. Soc.* **2003**, *125*, 1041−55.

vicinity of the Cu(II) facilitates, at least to some extent, electron transfer from **9** to O_2.

One may ask the question of whether the reaction of **9** and O_2 follows the same pathway as for the oxidative half-reaction in normal turnover, where it has been proposed that electron transfer from TPQ_{amr} (Scheme 1) occurs to a prebound O_2,[36] facilitated by the active-site Cu(II). In normal turnover, cofactor reoxidation for BPAO is characterized by low micromolar $K_m(O_2)$,[37] such that saturation is already achieved in normal aerobically equilibrated bulk solvent. In the case of autoxidation of **9**, however, the increased rate of the oxidative half-reaction in going from air exposure to pure O_2 exposure suggests that the mechanism of oxidation of **9** may be distinct from that used for oxidation of TPQ_{amr}. Alternatively, formation of adduct **9** may disrupt the normal binding site(s) for O_2.

Conclusion

To our knowledge, **1** is the first branched primary amine reported to act as a submicromolar K_i inhibitor of a quinone-dependent CAO yet is ultimately processed as a substrate. This activity is unique, first in that this family of enzymes is not known to metabolize branched primary amines, and there is only one other report (without characterization of the product) that a branched primary amine can be a substrate. Second, the finding of an enantioselective inhibitory potency is unprecedented, and if it represents stereoselective C_α deprotonation of the two possible substrate Schiff base epimers, the greater potency of (*S*)-**1** is consistent with the *pro-S* selectivity of C_α proton removal for benzylamine.

We chose to investigate the aminodihydrothiophene **1** on the basis of its tendency toward aromatization that might drive an initially reversible addition−elimination or transamination step. Since branched primary amines are not known as substrates for the quinone-dependent CAOs, we considered that an observed metabolism of **1** might occur by addition−elimination. We find that enzyme metabolism and a quinone model system both follow strictly a transamination course, consistent with what is now well established for unbranched primary amines.

We previously showed that an aromatization that can occur after transamination can result in a stable derivative of the CAO quinone cofactor in a form that is incapable of being reoxidized to generate the turnover-competent starting TPQ.[38] The series of inhibitors that satisfy this criterion, (3-aryl-)3-pyrrolines, was shown to result in stoichiometric inactivation of BPAO, forming a pyrrolylresorcinol TPQ derivative, though the same compounds are pure substrates of flavin-dependent MAO-B.[38] In the present work, kinetics and UV−vis spectrophotometric studies reveal that the initial quick inhibition of BPAO by (*S*)-**1** is due to formation of a derivative of the reduced cofactor upon a similar aromatization step. The striking difference between these two cases is that whereas the pyrrolylresorcinol cofactor is inert to further oxidation, the thiophenylaminoresorcinol cofactor is still subject to an albeit slow reoxidation and subsequent turnover, apparently facilitated by the active-site Cu(II), thereby rendering the observation of temporary rather than irreversible inactivation. From this point of view, compound **1** is an example of what can be termed mechanism-based *reversible* inactivation as opposed to the traditional competitive reversible inhibition or mechanism-based irreversible inactivation. Fine-tuning of the redox potential of the "coupling product" would theoretically permit control of the *duration* of inhibition independently of the *potency* of inhibition. This suggests a new concept in the design of enzyme inhibitors that may be applicable to a wide range of enzyme systems.

Experimental Section

General Procedures. All NMR experiments were run at ambient temperature, on a Varian Gemini 200 or 300 MHz instrument. Chemical shifts were referenced to the residual proton peaks in the deuterated solvents, and ^{13}C APT (attached proton test) designations are given as (+) or (−). Benzylamine assays were conducted on a Perkin-Elmer Lambda 3B instrument using the PECSS software, with constant temperature being maintained by a water-jacketed multiple cell holder. UV−vis spectra were recorded on a Perkin-Elmer Lambda 20 spectrophotometer. High-resolution mass spectra (HRMS) were obtained by electron impact ionization (EI) (20−40 eV) or fast atom bombardment (FAB) on a Kratos MS25RFA instrument. Ethyl 4-amino-4,5-dihydrothiophene-2-carboxylate (**1**), both as a mixture and as optically pure enantiomers, was synthesized according to a literature method.[13] The *S* enantiomer was prepared starting from the commercially available D-cysteine, which was first converted to its ethyl ester according to a literature method.[39] 5-*tert*-Butyl-2-hydroxy-1,4-benzoquinone (TBHBQ) and 5-*tert*-butyl-1,2,4-trihydroxybenzene (**7**) were prepared as described previously.[3b] Bovine plasma amine oxidase (BPAO) for inhibition assays (100 units/g of protein), glucose oxidase (245.9 units/mg of solid), and catalase (1870 units/mg of solid) were purchased from Sigma or Worthington. BPAO used for kinetics, HPLC, and UV−vis spectrophotometric studies was purified according a reported procedure.[5] The purified protein shows a single band on SDS−PAGE. Enzyme concentrations are in terms of active monomers as estimated from the rate of benzylamine oxidation (1 unit oxidizes 1.0 μmol of benzylamine to benzaldehyde per minute at 25 °C), using an activity of 0.48 unit/mg of protein for the pure monomer of molecular weight 85 000 and $\Delta\epsilon_{250} = 12\,800\ M^{-1}\ cm^{-1}$ for benzaldehyde [corresponding to an A_{250} of 12.8 min^{-1} (unit of activity)$^{-1}$ for 1 mL volume at 25 °C]. Concentrations measured this way are very close to those estimated by standard phenylhydrazine titration.[5] Stock solutions of **1** and **2** were prepared fresh by dilution with 0.1 M phosphate buffer, pH 7.2, of a 10 mM stock solution in pure water. The argon used for anaerobic experiments was deoxygenated and moisturized by passage sequentially through (1) a tower of V(II) [V_2O_5 dissolved in aqueous sulfuric acid in the presence of excess Zn(Hg)] and (2) a tower of aqueous $NaHCO_3$.

Kinetics of Aerobic Interaction of BPAO with 1. Solutions of BPAO and various concentrations of **1** in 0.9 mL of 0.1 M sodium phosphate buffer, pH 7.2, were incubated at 30 °C. Aliquots (100 μL) of the incubation mixture were withdrawn periodically and diluted into 1 mL of 5 mM benzylamine in 0.05 M sodium phosphate buffer, pH 7.2, at 30 °C (total volume 1.1 mL), and the BPAO activity was determined spectrophotometrically by monitoring the benzaldehyde production at 250 nm over the first 40 s. A control incubation lacking **1** was set up at the same time. Remaining enzyme activity (Figure 1) was calculated by comparison with the control.

To examine the reversibility of inactivation of BPAO by (*S*)-**1**, two solutions of 0.5 mL of BPAO (1.0 μM) in 0.1 M sodium phosphate buffer, pH 7.2, in the absence and presence of 50 μM (*S*)-**1** were incubated for 10 min, showing 64% remaining in the latter case. The two samples were then transferred into two dialysis membranes (6.4 mm Spectrum Spectro/Por membrane, MW cutoff 12 000−14 000) and dialyzed against 0.1 M sodium phosphate buffer, pH 7.2, at room temperature for 24 h. The enzyme activities of the two dialyzed samples were essentially identical.

(36) Su, Q.; Klinman, J. P. *Biochemistry* **1998**, *37*, 12513−12525.
(37) Oi, S.; Inamasu, M.; Yasunobu, K. T. *Biochemistry* **1970**, *9*, 3378−3383.
(38) Lee, Y.; Ling, K. Q.; Lu, X.; Silverman, R. B.; Shepard, E. M.; Dooley, D. M.; Sayre, L. M. *J. Am. Chem. Soc.* **2002**, *124*, 12135−12143.

Competitive Inhibition of BPAO by (*S*)-1. Solutions of BPAO (1.0 μM) in 0.1 M phosphate buffer, pH 7.2 (1 mL each), were incubated at 30 °C for 10 min before various concentrations of benzylamine and (*S*)-**1** were added simultaneously. After quick mixing, the solutions were subjected to spectrophotometric monitoring at 250 nm to yield slopes of PhCHO production over 40 s. Lineweaver−Burk and Dixon plots were constructed (Figure 3) to obtain inhibition constants.

Preparation of Ethyl 4-Aminothiophene-2-carboxylate (2) by Catalytic Dehydrogenation of 1. To a solution of **1**·HCl (181 mg, 1 mmol) in 100 mL of ethanol−benzene (1:1 v/v) were added triethylamine (420 μL, 3 mmol) and 10% Pd/C (40 mg). The mixture was heated at reflux for 4 h until TLC indicated total conversion of the starting material. Pd/C was filtered off and the filtrate was concentrated under reduced pressure. The residue was applied to a short silica gel column with hexanes/ethyl acetate (1:1) as eluant to afford the free base form of **2** (175 mg, 84%): light yellow oil; ^{1}H NMR ($CDCl_3$) δ 1.33 (t, 3H, J = 7.1 Hz), 3.67 (br s, 2H), 4.29 (q, 2H, J = 7.1 Hz), 6.37 (d, 1H, J = 1.8 Hz), 7.29 (d, 1H, J = 1.8 Hz); ^{13}C NMR (APT, $CDCl_3$) δ 14.4 (−), 61.2 (+), 107.8 (−), 126.0 (−), 132.8 (+), 145.5 (+), 162.3 (+); HRMS (FAB) calcd for $C_7H_9NO_2S$ 171.0354, found 171.0347. The sample was further converted to the HCl salt form by dissolution in 100 mL of ethanol followed by addition of concentrated aqueous HCl to pH 3. Removing solvent and crystallization of the residue from EtOH/EtOAc (1:4) afforded **2**·HCl as white crystals: mp 185−187 °C (decomp); ^{1}H NMR (CD_3OD) δ 1.38 (t, 3H, J = 7.1 Hz), 4.38 (q, 2H, J = 7.1 Hz), 7.78 (m, 1H), 7.85 (m, 1H).

TLC Detection of Turnover Product 2 in Metabolism of 1 by BPAO. A solution of 0.7 μM BPAO and 100 μM **1**·HCl (*R*,*S* mixture 63:37) in 1 mL of 0.1 M sodium phosphate buffer, pH 7.2, was incubated at 30 °C. A control incubation without BPAO was set up at the same time. After 24 h, the remaining enzyme activity was determined to be 20%. The incubation solution was then extracted with ethyl acetate (3 × 5 mL), and the organic extracts were combined, dried (Na_2SO_4), and evaporated to one drop. The residue was applied to a TLC plate, and the authentic **2** was loaded on the same plate. A mixture of CH_2Cl_2/MeOH (5:1) was used as eluent, and **2** was visualized by UV light (bright blue at 365 nm) or ninhydrin spray (dark pink color). The product and authentic **2** both showed identical spots with R_f = 0.3. No other products were apparent.

HPLC Monitoring of the Conversion of 1 to 2 Catalyzed by BPAO. A solution of 40 μM **1** (*R* or *S* enantiomer) and 0.7 μM BPAO in 1 mL of 0.1 M sodium phosphate buffer, pH 7.2, was incubated at 30 °C. Aliquots (100 μL) were taken periodically, and 50 μL of acetonitrile (containing 0.02% trifluoroacetic acid, TFA) was added to denature the enzyme. The resulting suspension was then centrifuged, and 20 μL fractions of the supernatant were subjected to HPLC analysis using a 4.6 × 250 mm Agilent SB C18, 5 μm column, a flow rate of 1 mL/min, and a gradient mobile phase composed of HPLC-grade solvents A [5% aqueous CH_3CN containing 0.02% (v/v) TFA] and B [95% aqueous CH_3CN containing 0.02% (v/v) TFA] according to the following program: 100% A to 93% A 0−20 min, 93% A to 50% A 20−25 min, 50% A to 100% A 25−30 min, 100% A 30−35 min. With this solvent program, compounds (*S*)-**1** and **2** had retention times of 11.8 and 12.5 min, respectively. The concentrations of (*S*)-**1** and **2** were determined according to their HPLC peak integrations (both monitored at 270 nm), calibrated according to independently established standard curves. The time-dependent plots for consumption of **1** and formation of **2** are shown in Figure 2. Nonlinear least-squares fits of the product formation plots were conducted by use of Origin 7.0 software according to the equation $[\mathbf{2}] = [\mathbf{2}]_\infty(1 - e^{-kt})$, where [**2**] and $[\mathbf{2}]_\infty$ represent the concentrations of product **2** during and at the end of reaction, respectively. A control run in the absence of the enzyme was set up at the same time. In a second control, compound **1** was incubated with the same amount of denatured enzyme [by addition of 10% (v/v) denaturing solution (2% 2-mecaptoethanol, 10% glycerol, and 4% SDS] and heating for 6 min at 100 °C). No product **2** was detected in either control experiment.

UV Spectrophotometric Monitoring of BPAO-Catalyzed Conversion of (*S*)-1 to 2. A solution of (*S*)-**1** (50 μM) and BPAO (1.6 μM) in 0.1 M sodium phosphate buffer, pH 7.2, in an open quartz cuvette (1 cm) was monitored at 30 °C by repetitive spectral scan at 6 min time intervals. Difference spectra were then generated by Origin 7.0 by subtracting the first spectrum from all the spectra recorded thereafter (Figure S1 in Supporting Information).

Anaerobic Reaction of 1 with 5-*tert*-Butyl-2-hydroxy-1,4-benzoquinone in DMSO. To a solution of TBHBQ (90 mg, 0.5 mmol) and **1**·HCl (105 mg, 0.5 mmol) in 5 mL of degassed DMSO was added degassed diisopropylethylamine (DIPEA, 350 μL, 2 mmol). The solution was stirred for 20 h under argon and then quenched by adding 3.5 mL (25 mmol) of degassed triethylamine and 2 mL (21 mmol) of degassed acetic anhydride. The resultant mixture was stirred at room temperature for 2 h and partitioned between 100 mL of water and 100 mL of CH_2Cl_2. The organic layer was separated, washed with water (3 × 50 mL), dried (Na_2SO_4), and concentrated, and the residue was subjected to flash silica gel column chromatography with hexanes−EtOAc as eluent to afford three acetylated products:

Monoacetylated 2 [ethyl 4-(acetamido)thiophene-2-carboxylate, 37 mg, 35%]: light brown solid; mp 104−106 °C; ^{1}H NMR ($CDCl_3$) δ 1.37 (t, 3H, J = 7.1 Hz), 2.17 (s, 3H), 4.34 (q, 2H, J = 7.1 Hz), 7.65 (d, 1H, J = 1.5 Hz), 7.78 (br s, 1H, NH), 7.81 (d, 1H, J = 1.5 Hz); ^{13}C NMR ($CDCl_3$) δ 14.3, 23.9, 61.4, 117.3, 126.2, 132.3, 135.9, 162.1, 167.9; HRMS (FAB) calcd for $C_9H_{12}NO_3S$ (MH^+) 214.0538, found 214.0539.

Triacetylated 6 [ethyl 4-(*N*-(2,4-diacetoxy-5-*tert*-butylphenyl)acetamido)thiophene-2-carboxylate, 135 mg, 58%]: light brown gummy solid; mp 50−52 °C; ^{1}H NMR ($CDCl_3$) δ 1.28 (t, 3H, J = 7.2 Hz), 1.30 (s, 9H), 1.95 (s, 3H), 2.07 (s, 3H), 2.29 (s, 3H), 4.25 (q, 2H, J = 7.2 Hz), 7.01 (s, 1H), 7.25 (br s, 1H), 7.30 (br s, 1H), 7.64 (d, 1H, J = 2.0 Hz); ^{13}C NMR (APT, $CDCl_3$) δ 14.3 (−), 20.5 (−), 21.6 (−), 23.5 (−), 30.1 (−), 34.6 (+), 61.3 (+), 120.1 (−), 121.3 (−), 128.1 (−), 129.2 (−), 131.2 (+), 132.0 (+), 140.0 (+), 141.0 (+), 144.8 (+), 149.1 (+), 161.8 (+), 168.2 (+), 168.5 (+), 170.1 (+); HRMS (FAB) calcd for $C_{23}H_{27}NSO_7$ (MH^+) 462.1586, found 462.1575.

Triacetylated 7 (1,2,4-triacetoxy-5-*tert*-butylbenzene,[40] 51 mg, 33%): white crystals; mp 118−119 °C; ^{1}H NMR ($CDCl_3$) δ 1.33 (s, 9H), 2.26 (s, 3H), 2.28 (s, 3H), 2.32 (s, 3H), 6.97 (s, 1H), 7.15 (s, 1H); ^{13}C NMR (APT, $CDCl_3$) δ 20.7 (−), 21.6 (−), 30.0 (−), 34.5 (+), 119.0 (−), 121.6 (−), 139.0 (+), 139.76 (+), 139.81 (+), 146.3 (+), 168.0 (+), 168.3 (+), 168.9 (+).

The same reaction was repeated but with omission of the acetic anhydride trapping step. The final product mixture was carefully separated by column chromatography using hexanes/ethyl acetate as eluent to give products **2** (30 mg, 35%) and **6** (88 mg, 52%). Compound **2** (free base form) was identical with an authentic sample as shown by NMR and HPLC. Triol **7** was autoxidized to TBHBQ during workup and was not recovered.

Ethyl 4-((5-*tert*-Butyl-2,4-dihydroxyphenyl)amino)thiophene-2-carboxylate (6): brown amorphous solid; mp 73−75 °C; ^{1}H NMR ($CDCl_3$) δ 1.35 (s, 9H), 1.36 (t, 3H, J = 7.1 Hz), 4.33 (q, 2H, J = 7.1 Hz), 5.11 (br s, 1H), 5.25 (br s, 1H), 5.92 (br s, 1H), 6.29 (d, 1H, J = 1.8 Hz), 6.40 (s, 1H), 7.03 (s, 1H), 7.36 (d, 1H, J = 1.8 Hz); ^{13}C NMR (APT, DMSO-d_6) δ 14.2 (−), 29.8 (−), 33.8 (+), 60.7 (+), 104.2 (−), 104.4 (−), 119.5 (−), 121.7 (+), 125.9 (+), 126.1 (−), 130.7 (+), 146.7 (+), 147.5 (+), 151.4 (+), 161.6 (+); HRMS (FAB) calcd for $C_{17}H_{21}NO_4S$ (M^+) 335.1191, found 335.1188.

NMR Tube Reaction of 1 with TBHBQ. To a 5 mm NMR tube containing a solution of **1**·HCl (10.6 mg, 0.05 mmol) and TBHBQ

(39) Meng, Q.; Li, Y.; He, Y.; Guan, Y. *Tetrahedron: Asymmetry* **2000**, *21*, 4255−4261.
(40) Blatchly, J. M.; Green, R. J. S.; McOmie, J. F. W. *J. Chem. Soc., Perkin Trans. 1* **1972**, 2286−2291.

(9.0 mg, 0.05 mmol) in 0.7 mL of degassed DMSO-d_6 at room temperature was added DIPEA (35 μL, 0.2 mmol) to initiate the reaction. The ^{1}H NMR spectra were recorded periodically over 20 h. After completion of the reaction, the presence of peaks corresponding to **2** and **6** was confirmed by spiking with authentic samples. Time-dependent plots for consumption of TBHBQ and formation of **2** and **6** were constructed based on integrations of well-separated characteristic ^{1}H NMR signals (the quinone peak at 6.06 ppm for TBHBQ; the thiophene peak at 6.38 ppm for **2**; and the thiophene peak at 7.45 ppm for **6**). Since the reaction was essentially stoichiometric and the amounts of **2** and **7** were identical, the total integration of TBHBQ, **2**, and **6** was counted as 100 and the percentages of each of the three components were calculated and plotted over time (Figure 4).

Preparation of *N*-(2-(Ethoxycarbonyl)thiophen-4-yl)-2-hydroxy-5-*tert*-butyl-1,4-benzoquinone-1-imine (8). A mixture of **6** (32 mg, 0.1 mmol) in 10 mL of CH_3CN/pH 7.2 phosphate buffer (5:1) was stirred for 12 h at room temperature and then extracted with CH_2Cl_2 (3 × 30 mL). The combined organic extract was dried (Na_2SO_4) and concentrated, and the residue was subjected to flash column chromatography with hexanes/EtOAc (1:1) as eluent to afford **8** (18 mg, 55%): red crystals; mp 123−125 °C; ^{1}H NMR ($CDCl_3$) δ 1.26 (s, 9H), 1.40 (t, 3H, J = 4.8 Hz), 4.39 (q, 2H, J = 4.8 Hz), 5.99 (s, 1H), 7.00 (s, 1H), 7.20 (d, 1H, J = 1.0 Hz), 7.64 (d, 1H, J = 1.0 Hz); ^{13}C NMR ($CDCl_3$, APT) δ 14.4 (−), 29.6 (−), 35.9 (+), 61.8 (+), 108.2 (−), 119.1 (−), 122.2 (−), 129.1 (−), 135.1 (+), 146.0 (+), 153.5 (+), 154.7 (+), 157.3 (+), 161.6 (+), 187.8 (+); HRMS (EI) calcd for $C_{17}H_{19}NO_4S$ (M^+) 333.1035, found 333.1032.

Autoxidation of 6 and Hydrolysis of 8. A solution of **6** (0.15 mM) in 3 mL of 1:1 (v/v) DMSO and 0.05 M 4-(2-hydroxyethyl)-1-piperazineethanesulfonate (HEPES) buffer, pH 7.2, in an open quartz cuvette (1 cm) was monitored at 25 °C by repetitive spectral scan on a UV−vis spectrophotometer at 20 min time intervals (Figure 5). The recorded spectra were analyzed with Origin 7.0. The pseudo-first-order kinetic constants for autoxidation and hydrolysis were obtained from linear fits of ln $[(A_\infty - A_0)/(A_\infty - A_t)]$ versus t plots (Figure 5, insets), where A_0, A_t, and A_∞ represent A_{490} (autoxidation) and A_{420} (hydrolysis) at the beginning, during, and at the end of the inspected reactions. Appropriate A_∞ values were chosen to allow best linear fits of the plots, which were close to the theoretical values predicted from the UV−vis spectrum of authentic **8**. In another experiment, the same incubation was conducted in the presence of 0.1 mM DTPA sodium salt, affording essentially the same kinetic constants after the same data analysis. In a third experiment, a solution of authentic **8** (0.15 mM) in 1:1 (v/v) DMSO and 0.05 M HEPES buffer, pH 7.2, was subjected to UV−vis spectrophotometric monitoring as above. The spectra obtained were treated similarly to yield a hydrolysis rate constant close to that obtained above.

To confirm the formation of TBHBQ and **2** in the above reaction, a solution of **6** (0.2 mM) in neat 0.05 M HEPES buffer, pH 7.2 (20 mL), was stirred in air at room temperature overnight. The resulting red solution was divided equally into two parts. The first half was acidified with 6 N aqueous HCl to pH 1, saturated with NaCl, and then extracted with Et_2O (2 × 10 mL). The combined organic layer was dried (Na_2SO_4), concentrated, and examined by TLC, showing the presence of TBHBQ as compared with an authentic sample. The second half of the above reaction mixture was directly saturated with NaCl and extracted with Et_2O (2 × 10 mL). TLC analysis of the dried and concentrated organic layer indicated the presence of **2** as compared with an authentic sample.

Cu(II)-Mediated Autoxidation of 6. To a solution of **6** (0.15 mM) in 3 mL of 1:1 (v/v) DMSO and 0.05 M HEPES buffer, pH 7.2, in an open quartz cuvette (1 cm) was added 9 μL of 50 mM aqueous $CuSO_4$. After quick mixing, the solution was subjected to UV−vis monitoring in air at 25 °C. The reaction exhibited no further spectral changes over a period of 24 h after the first spectrum was recorded after 1 min (Figure S2 in Supporting Information). To the resulting reddish-yellow solution was added 18 μL of 50 mM aqueous DTPA. The solution was mixed and subjected to repetitive UV−vis spectral scan, showing release of **8** within 1 min (Figure S2 in Supporting Information). Hydrolysis of **8** to form TBHBQ and **2** was evident following overnight standing of the solution.

To determine the rate constant of Cu(II)-mediated autoxidation of **6** to **8**−Cu(II), the above reaction was repeated with 0.1 mM **6** and 0.1 mM Cu(II). After quick mixing, the absorbance at 390 nm was monitored at 25 °C over time (Figure S3 in Supporting Information). The pseudo-first-order rate constant was calculated by a double-variable nonlinear least-squares fit of the A_{390} versus t plot with Origin 7.0 according to the equation $A_t = A_\infty - (A_\infty - A_0)e^{-kt}$, where A_0, A_t, and A_∞ represent A_{390} at the beginning, during, and at the end of the reaction. The A_∞ obtained was close to the theoretical value predicted from the UV−vis spectrum of authentic **8**−Cu(II).

Kinetic Studies on Stoichiometric Reactions of BPAO with (*S*)-1. For aerobic reactions, a solution of BPAO (1.0 μM, 1.1 mL) in 0.1 M sodium phosphate buffer, pH 7.2, was incubated at 30 °C for 10 min and then a 100 μL aliquot was withdrawn and assayed to establish the control activity. An independent experiment indicated that the enzyme activity remained constant at least for several hours. To the above BPAO solution was added 5 μL of 0.24 mM aqueous (*S*)-**1** (1.2 equiv) at 30 °C. After quick mixing of the solution, aliquots (100 μL each) were periodically assayed to afford the time-dependent enzyme activity plot (Figure 6, left panel).

For anaerobic inactivation, a solution of BPAO (1.0 μM, 1.1 mL) in 0.1 M sodium phosphate buffer, pH 7.2, was prepared in a 10 mL culture tube and then sealed with a septum. An inlet needle was used to connect the culture tube to a deoxygenated humidified argon gas line. An outlet needle was also attached to the septum. The solution was incubated at 30 °C while a slow argon stream was directed at the top of the solution for 3 h. The outlet needle was then removed to maintain a positive argon pressure within the culture tube. A 100 μL aliquot was withdrawn and assayed to give the control enzyme activity. After injection of 5 μL of degassed 0.24 mM aqueous (*S*)-**1**, the incubation solution was quickly mixed and the enzyme activity was assayed over time (Figure 6, left panel).

To measure the O_2-dependent activity recovery of anaerobically inactivated BPAO, 2 mL samples of enzyme (1.0 μM) were anaerobically inactivated as above for 60 min by (*S*)-**1** (1.2 μM) in a culture tube. The septum was removed and the enzyme solution was bubbled either with air or with O_2 for 10 s. The solutions were then assayed over time, yielding the time-dependent activity plot (Figure 6, right panel). The enzyme activity recovery plots were analyzed with Origin 7.0 by double-variable (k and Act_∞) pseudo-first-order nonlinear least-squares fits according to equation $Act_t = Act_\infty - (Act_\infty - Act_0)e^{-kt}$, where Act_0, Act_t, and Act_∞ represent the remaining enzyme activities at the beginning, during, and at the end of the O_2-dependent activity recovery. The results are shown in Table 1.

HPLC Analysis of Stoichiometric Reactions of BPAO with (*S*)-1. All the incubations were conducted at room temperature in 5 mm NMR tubes cut to 10 cm in length. A solution of BPAO (100 μM) in 0.1 M sodium phosphate buffer, pH 7.2 (40 μL), was prepared in a septum-sealed NMR tube and made anaerobic by directing a slow argon stream at the top of the solution for 3 h before 10 μL of degassed 0.5 mM aqueous (*S*)-**1** was injected. The reaction mixture was incubated under argon for 30 min and then 10 μL of degassed 20% aqueous trichloroacetic acid (TCA) was injected, resulting in immediate precipitation of the protein. After centrifugation of the solution for 5 min, the supernatant (20 μL) was withdrawn and subjected to HPLC analysis as described above, showing the absence of (*S*)-**1**. The concentration of **2** thereby determined was converted to yield based on starting (*S*)-**1**.

For the same reaction under strictly anaerobic conditions, a solution of BPAO (100 μM), glucose oxidase (60 μg/mL), and catalase (60 μg/mL) in 0.1 M sodium phosphate buffer, pH 7.2 (40 μL), was purged

with argon for 3 h and then 1 μL of degassed 1 M aqueous glucose was added. After further argon purging for 1 h, 10 μL of degassed 0.5 mM aqueous (*S*)-**1** was injected and the mixture was incubated for 30 min before TCA workup and HPLC analysis. A control experiment in the absence of BPAO showed 100% recovery of (*S*)-**1**.

To examine the recovery of **2** after complete turnover of (*S*)-**1** by BPAO, a solution of BPAO (100 μM) in 0.1 M sodium phosphate buffer, pH 7.2 (40 μL), was purged with argon for 3 h and appropriate amounts of (*S*)-**1** were injected. The reaction mixture was incubated for 30 min and then exposed to pure O_2 for 1 h before TCA workup and HPLC analysis. In one of these experiments, 10 μL of degassed denaturing solution composed of guanidine hydrochloride (7 M) and β-mercaptoethanol (30 mM) was injected at the end of O_2 exposure. The mixture was heated at 90 °C for 5 min and subjected to normal TCA workup and HPLC analysis.

To examine the recovery of **2** following its direct incubation of BPAO, a solution of BPAO (100 μM) in 0.1 M sodium phosphate buffer, pH 7.2 (40 μL), was purged with argon for 3 h and **2** was added to a final concentration of 100 μM. The reaction mixture was incubated for 30 min and worked up and analyzed as above.

General Procedure for UV−Vis Spectrophotometric Monitoring of Anaerobic Experiments with BPAO. All experiments were conducted with a 1 mm quartz cuvette at 25 °C. Preparation of anaerobic protein samples for spectrophotometry first involved slow filtering of the enzyme solution (to remove any insoluble materials and ensure good spectral quality) into a 10 mL culture tube, which was then sealed with a septum and attached to the deoxygenated humidified argon gas line by an inlet needle. A long needle was applied to connect the culture tube to a septum-sealed 1 mm quartz cuvette, to which an outlet needle was also attached. After slow streaming of argon at the top of the solution for 3 h, the end of the long needle attached to the culture tube was pushed down to the bottom and the other end of the long needle attached to the cuvette was pulled up to an appropriate level, thereby allowing the argon pressure to slowly drive the protein solution from the culture tube into the cuvette. To ensure anaerobic conditions, positive argon pressure was maintained within the cuvette throughout the spectrophotometric measurements.

When difference UV−vis spectra were generated to pick up weak signals of the enzyme cofactor from the protein background, volume changes of the solution upon each addition of reagents were corrected by use of Origin 7.0 to avoid artifacts in the region (∼280 nm) of strong absorption of the protein. To ensure good resolution of the difference spectra, concentrations of BPAO were used that kept A_{280} less than 2.5. In generating the difference spectra for model reactions, the absorbances of all the original UV−vis spectra (Figure S4 in Supporting Information) were converted to extinction coefficients (ϵ) by use of Origin 7.0.

UV−Vis Spectrophotometric Monitoring of Reactions of BPAO with (*S*)-1. An anaerobic solution of BPAO (80 μM) in 0.1 M sodium phosphate buffer, pH 7.2 (300 μL), was prepared and transferred to a septum-sealed 1 mm quartz cuvette. The UV−vis spectrum was recorded, and the enzyme activity was assayed (2 μL aliquot). Into this solution was injected 10 μL of degassed 2.4 mM aqueous (*S*)-**1**. After the sample was mixed carefully for 2 min, the enzyme activity was assayed and the UV−vis spectrum was taken again, at which point the TPQ chromophore had disappeared (Figure S5 in Supporting Information). An O_2 stream was directed at the solution for 1 min and an O_2 balloon was fitted to the cuvette prior to repetitive UV−vis spectral scanning at 10 min intervals for 2 h (Figure S6 in Supporting Information), with periodic monitoring of the enzyme activity. The resulting reddish-yellow enzyme sample was transferred into a dialysis membrane and subjected to dialysis for 24 h against 0.1 M sodium phosphate buffer, pH 7.2 (3 × 250 mL). The activity was assayed and the UV−vis spectrum was taken (Figure S9 in Supporting Information).

The same reaction was repeated in the presence of glucose oxidase (33 μg/mL), catalase (33 μg/mL), and glucose (17 mM). The difference spectrum for the reductive half-reaction (not shown) was essentially the same as that in the absence of glucose/glucose oxidase/catalase. However, it took a much longer time (∼12 h rather than 2 h) for restoration of the TPQ chromophore on account of consumption of O_2 at the expense of glucose oxidation and the slow diffusion of gas into the viscous solution.

Aerobic Titration of BPAO with 2. A solution of BPAO (80 μM) in 0.1 M sodium phosphate buffer, pH 7.2 (300 μL), in a 1 mm quartz cuvette was titrated with 0.6 mM aqueous **2** (10 μL each), and the UV−vis spectra were recorded accordingly (Figure S10 in Supporting Information).

Acknowledgment. We thank Doreen Brown for purification of BPAO used in this work and Nicole Samuels (J. P. Klinman lab) for helpful discussions about chemical reduction of the enzyme cofactor. We are grateful for support of this work by the National Institutes of Health through Grants GM 48812 (L.M.S. and D.M.D.) and GM 27659 (D.M.D.).

Supporting Information Available: Additional figures and experimental details. This material is available free of charge via the Internet at http://pubs.acs.org.

JA058838F